

Natural Radon and Radium Isotopes for Assessing Groundwater Discharge into Little Lagoon, AL: Implications for Harmful Algal Blooms

Ni Su · William C. Burnett · Hugh L. MacIntyre ·
Justin D. Liefer · Richard N. Peterson · Richard Viso

Received: 21 March 2013 / Revised: 28 September 2013 / Accepted: 20 October 2013 / Published online: 8 November 2013
© Coastal and Estuarine Research Federation 2013

Abstract Naturally occurring isotopes of radon (^{222}Rn) and radium isotopes ($^{223,224,226,228}\text{Ra}$) were used as tracers to assess submarine groundwater discharge (SGD) into Little Lagoon, AL (USA), a site of recurring harmful algal blooms (HABs). The radium isotopic data suggests that there are two groundwater sources of these tracers to the lagoon, a shallow (A1) and deeper (A2) aquifer. We estimated the fraction of each source via a three-end-member mixing model consisting of Gulf of Mexico seawater, shallow and deep groundwater. The estimated lagoonwide SGD rates based on a radium mass balance and the mixing model were 1.22 ± 0.53 and $1.59 \pm 0.20 \text{ m}^3 \text{ s}^{-1}$ for the shallow and deep groundwater discharges, respectively. To investigate temporal variations in SGD, we performed several radon surveys from 2010 through 2012, a

period of generally declining groundwater levels due to a drought in the southeastern USA. The total SGD rates based on a radon mass balance approach were found to vary from 0.60 to $2.87 \text{ m}^3 \text{ s}^{-1}$. We observed well-defined relationships between nutrients and chlorophyll-*a* in lagoon waters during a period when there was an intense diatom bloom in April 2010 and when no bloom existed in March 2011. A good correlation was also found between radium (groundwater-derived) and nutrients during the April 2010 period, while there was no clear relationship between the same parameters in March 2011. Based on multivariate analysis of chemical and environmental factors, we suggest that nutrient-rich inputs during high SGD may be a significant driver of algal blooms, but during low SGD periods, multiple drivers are responsible for the occurrence of algal blooms.

Communicated by Craig Tobias

Electronic supplementary material The online version of this article (doi:10.1007/s12237-013-9734-9) contains supplementary material, which is available to authorized users.

N. Su · W. C. Burnett (✉)
Department of Earth, Ocean and Atmospheric Sciences, Florida State University, Tallahassee, FL 32306, USA
e-mail: wburnett@fsu.edu

N. Su
State Key Laboratory of Estuarine and Coastal Research, East China Normal University, Shanghai 200062, People's Republic of China

H. L. MacIntyre
Department of Oceanography, Dalhousie University, PO Box 15000, Halifax, NS B3H 4R2, Canada

J. D. Liefer
Dauphin Island Sea Lab, 102 B Bienville Blvd, Dauphin Island, AL 36528, USA

R. N. Peterson · R. Viso
Center for Marine and Wetland Studies, Coastal Carolina University, Conway, SC 29526, USA

Keywords Radium isotopes · Radon · Submarine groundwater discharge · Algal blooms · Little Lagoon · Alabama

Introduction

Submarine groundwater discharge (SGD) is the flow of water on continental margins from the seabed to the coastal ocean, regardless of fluid composition or driving force (Burnett et al. 2003a). SGD consists of the direct freshwater flow from an aquifer to the ocean as well as the mixtures of freshwater–seawater cycling through surficial unconfined and deeper semi-confined aquifers (Moore 2010). The required conditions for the occurrence of terrestrial groundwater flow toward the sea are that an aquifer is hydraulically connected to the sea and that the water table lies above the adjacent mean sea level (Burnett et al. 2006). Tidal pumping, convection, bioturbation, and other processes also contribute to exchange between pore fluids in sediments and the overlying coastal seawater (Santos

et al. 2008a). The extent of SGD in coastal waters can be determined using naturally occurring radon (^{222}Rn) and radium isotopes ($^{223,224,226,228}\text{Ra}$). These are effective SGD tracers as they behave conservatively in seawater, are higher in concentration in groundwater relative to surface water, and their decay rates vary over both the long and short time-scale processes in question (Burnett & Dulaiova 2003; Burnett et al. 2008; Santos et al. 2008b).

Interest in SGD has been growing due to the recognition of its relative importance to water balance on land and the contribution to coastal ocean biogeochemistry via input of nutrients and other species (Valiela et al. 1990; Laroche et al. 1997). In certain locations, the transport of land-derived chemical species through SGD can rival that delivered via local river runoff (Burnett et al. 2003a; Slomp & Van Cappellen 2004; Swarzenski et al. 2006b; Swarzenski et al. 2007) and contribute to coastal water eutrophication, resulting in ecological or human health problems (Valiela et al. 1990; Charette et al. 2001; Lee & Kim 2007). For example, dinoflagellate blooms occurring in the southern Sea of Korea appear to be related to nutrient-enriched groundwater supply (Lee & Kim 2007; Lee et al. 2010). Hu et al. (2006) suggested that blooms of the toxic dinoflagellate *Karenia brevis* in the Gulf of Mexico (GOM) are supported in part by SGD along the west Florida coast due to the intense rains associated with numerous hurricanes that occurred prior to the blooms. Groundwater discharge has been argued both to militate against (LaRoche et al. 1997) and stimulate (Gobler & Sañudo-Wilhelmy 2001) blooms of the “brown tide” pelagophyte *Aureococcus anophagefferens* in shallow estuaries on Long Island, NY (USA).

In the present work, we report on our investigations of Little Lagoon (Baldwin County, AL, USA), a hot-spot for toxic blooms of the HAB diatom *Pseudo-nitzschia* spp. Liefer et al. (2009) showed that the density of these blooms is highly correlated with discharge from the surficial aquifer. In that study, relative SGD rates were inferred from discharge of the Styx River into Perdido Bay as both the river and the lagoon are connected to the same aquifer. Here we report direct assessments of SGD in Little Lagoon (LL) via isotopic approaches. The main objectives of this study are to discern the patterns and amounts of SGD in LL by using natural radioisotopes and to investigate possible relationships between SGD, nutrient concentrations and the occurrence of algal blooms.

Materials and Methods

Site Description and Approach

Little Lagoon is a shallow enclosed coastal lagoon with an average water depth of ~1.5 m and a surface area of 10.52 km²

in Baldwin County, AL (USA) (Fig. 1). A small brackish-water lake, Lake Shelby (LS), in the eastern part of the study area is connected to the lagoon through the Lake Shelby canal (hereafter LS canal). Another canal not connected to LS drains into the northeast section of the lagoon (hereafter NE canal). The lagoon is connected to the GOM and experiences tidal exchange via Little Lagoon Pass (LLP), a single shallow (~1-m-deep) and narrow (~10-m-wide) pass. This pass was closed from late May through July 2010 to prevent oil from the Deepwater Horizon spill from entering the lagoon. Irregular diurnal tides have a mean range outside the lagoon of ~0.5 m and damped tides inside of only ~0.15 m. The lagoon lacks stream inputs but likely receives significant groundwater inputs from the surficial aquifer because of a local maximum in groundwater elevation (Dowling et al. 2004; Murgulet & Tick 2008, 2009). The unconfined aquifer (A1 aquifer, ~30 m thick) here is typical of coastal plain deposits throughout much of the GOM consisting of fine- to coarse-grained quartz sands, with varying degrees of heavy minerals, shell fragments, and silt. The primary source of recharge for this aquifer comes from local precipitation (average annual precipitation = 167 cm year⁻¹) infiltrating the surface sands (Dowling et al. 2004). The confined aquifer (A2 aquifer, 60 to 75 m thick) is composed of (i) nonfossiliferous fine to medium reddish brown sands with thin, discontinuous lenticular beds of clay, and (ii) micaceous, fine- to coarse-grained quartz sands, with some ironstone and minor laminated clay layers (Chandler et al. 1985).

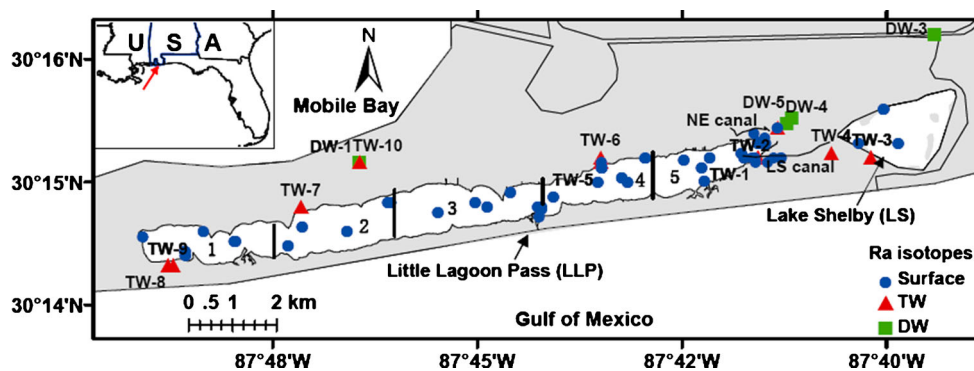
Measurements of Radon and Radium Isotopes in Water

We performed field investigations from April 2010 to August 2012. Our general strategy consisted of: (1) conducting radon surveys in near-surface waters along the shoreline of LL and LS to qualitatively locate points of enhanced SGD and to quantify the temporal variation in SGD rates; (2) sampling groundwater for Rn and Ra isotopes and nutrient concentrations to determine end-member groundwater concentrations; and (3) sampling lagoon surface waters for Ra isotopes, nutrient concentrations and chlorophyll to estimate quantitatively the water residence time and SGD rates for comparison to Rn-derived SGD estimates.

Surface water samples (ca. 60l) were collected for radium isotope analysis from LL, LS, canals (C), and groundwater wells around the lagoon (Fig. 1). Analyses of well waters were conducted by sampling from deep wells (DW, mostly used for irrigation purposes) in the A2 aquifer. We installed some shallow “tube wells” (TW) around the lagoon later in the study using narrow (diameter ~ 6 cm) PVC pipes inserted 1–4 m into the A1 aquifer.

Radium isotopes were pre-concentrated by adsorption onto Mn impregnated acrylic fibers (Mn-fibers) using standard techniques (Moore 1976). After extraction, the fibers were

Fig. 1 Little Lagoon, AL, with surface water and groundwater sampling stations. The vertical lines separate the lagoon into five segments (1–5), which are used for calculating volume-weighted radioisotope activities



washed thoroughly with radium-free tap water to remove residual salt and particles. In the laboratory, the moisture of the Mn-fibers was adjusted with a stream of compressed air, and the activities of short-lived radium isotopes (^{223}Ra and ^{224}Ra) were measured using a delayed-coincidence counting system (RaDeCC) described by Moore and Arnold (1996). Activities of ^{224}Ra were corrected for that supported by its parent ^{228}Th , so ^{224}Ra reported here are all “excess” activities.

After the measurements of the short-lived Ra isotopes (^{223}Ra and ^{224}Ra) were completed, the fibers were placed into gas-tight cartridges, stored for about 5 days for ^{222}Rn ingrowth, and then radon was transferred into Lucas cells via a radon emanation line for determination of ^{226}Ra (Peterson et al. 2009). Samples were next processed for the analysis of both long-lived Ra isotopes (^{226}Ra and ^{228}Ra) using an Ortec IG detector with a relative efficiency of 20 % (Dulaiova & Burnett 2004). Mn-fibers were packed into custom-made stainless-steel crucibles (0.05 mm thick, MSC Industrial Supply) and ashed at 600°C for 6 h in a muffle furnace. The crucibles were then folded first by hand, hydraulically pressed using 1 kg cm⁻² pressure with a hand press, and sealed with a silicone sealant to create a ~3-mm-thick counting wafer. In this process, the crucible serves as the counting vessel which eliminates any transfer steps between containers. Taking into any gamma ray absorption by the stainless steel, we calibrated the system by measuring the standards that were produced in the same way. After aging to allow ingrowth of ^{222}Rn daughters, the ^{226}Ra activity was estimated from ^{214}Pb and ^{214}Bi photopeaks (295, 352, and 609 keV), while ^{228}Ra activity was estimated using photopeaks of ^{228}Ac (338 and 911 keV). There was good agreement between ^{226}Ra determined via Lucas cell counting and assessed by gamma spectrometry ($R = 0.97$, $n = 112$). The values reported in this work are from the Lucas cell determinations which have better precision.

Radon surveys were performed along the shore of the lagoon, the shore of LS and in the NE and LS canals. Activities of ^{222}Rn in the lagoon surface waters were measured continuously using an automated pumping and sparging system connected to a suite of three RAD-7 detectors arranged with the counting cycles time-parallel for real-time in situ analysis (Burnett et al. 2001; Dulaiova et al. 2005). The

cruising speed was ~3–5 km h⁻¹. The counting interval was set to generally 5 min. The radon system is integrated with a CTD Diver (Van Essen) and logging GPS with depth-sounding capabilities. Radon concentrations in discrete samples of deep and shallow groundwater were measured on 250-ml grab samples using an additional radon-in-water (RAD-H2O) accessory (Durrige) to the RAD7 radon detector. Before taking a grab sample from a well, the well water was purged first for ~10–20 min in order to remove the stagnant well water. Later, the grab bottles were filled with care to prevent radon loss.

Radium in Sediment Measurements

On March 9, 2011, five sediment samples were collected along a transect spanning the entire lagoon. After drying and homogenizing the sediments, they were packed into gas-tight 100 cm³ aluminum cans. After >3 weeks for radon ingrowth, the samples were measured for ^{226}Ra and ^{228}Ra activities on the same Ortec germanium detector and using the same photopeaks as used for the radium-in-water measurements. The germanium detector was calibrated against a series of IAEA natural matrix standards prepared with the same geometry.

Nutrient Measurements

Water samples for nutrient analyses were collected from groundwater wells in parallel with all groundwater radioisotope measurements. Samples for nutrient analyses were also collected in parallel with all surface water radium measurements and at discrete points along each radon survey transect. Samples were collected in acid-washed polyethylene bottles and kept in a cooler on ice until processing. Samples were filtered through Whatman GF/F filters (0.7 μm) with gentle vacuum pressure (<17 kPa or 5" Hg). The filtrate was collected in acid-washed high-density polyethylene flasks for analysis of dissolved components and frozen until analysis. Aliquots for measurement of total nutrients were collected and frozen immediately.

The filtrate samples were analyzed colorimetrically using a Skalar Sans 10 autoanalyzer for dissolved inorganic nitrogen (DIN = the sum of nitrate, nitrite, and ammonium), phosphate, and silicate. Total dissolved nitrogen (TDN) and total nitrogen (TN) were also determined colorimetrically as nitrate using the autoanalyzer after oxidation with potassium persulfate (Valderrama 1981). Dissolved organic nitrogen (DON) was determined as the difference between DIN and TDN. Total phosphorus (TP) was determined colorimetrically following acid hydrolysis (Solórzano & Sharp 1980).

Resistivity Measurements

Electrical resistivity data in LL and LS were collected on September 28–29, 2010 using an AGI Supersting R8 eight-channel resistivity apparatus. The meter was programmed for continuous resistivity profiling (CRP) with a dipole–dipole survey geometry. A floating streamer with 12-m electrode spacing and a total length of 96 m was towed behind the boat. The current injection electrodes were positioned 10 m behind the survey boat to avoid any interference from the boat. The injection electrodes impart an electrical field sampled by successive pairs of receiver electrodes for voltage drops. Increasing offset between the electrodes results in increased depth of sampling. The full depth of penetration is nominally one third of the streamer length or about 30 m in this case. This was considered ideal for penetrating a shallow water column and imaging the resistivity structure of the shallow aquifer system such as that underlying LL.

Raw electrical soundings were integrated with depth and location from a Lowrance depth finder and GPS unit (Model HDS5). Proper positioning and depth information provide constraints for inversion modeling to negate the effects of the water layer overlying the sediments. Data were inverted with AGI's EarthImager 2D software. An iterative approach between the modeled resistivity structure and the raw electrical soundings results in color-contoured electrical resistivity tomograms (Fig. 2). Iterations are complete when least squares difference and root mean square errors meet acceptable thresholds demonstrating <10 % difference between modeled and raw soundings. Conditions were calm and clear during data collection and no significant environmental noise (e.g., large electrically conductive bodies) was visually observed.

Results

Resistivity Structure in the LS and LL Aquifer

Conductivity (the inverse of resistivity) is typically different in groundwaters than associated surface waters and thus may be used as an indicator of interactions between these water

masses. In principle, resistivity responds to differences in sediment characteristics, water content, and amount of dissolved materials within the pore water (Swarzenski et al. 2006a; Taniguchi et al. 2007). Higher resistivity corresponds to lower salinity of the pore solutions in the saturated sediment, assuming that the sediment characteristics (e.g., porosity) are homogeneous. In order to identify groundwater sources and discharge zones in our study area, apparent electrical resistivity was measured along the near-shore portion of the lagoon and LS to provide images of subsurface resistivity structure for pore waters shallower than 30 m. For the resistivity profile along the southeast shore of the lagoon, it very much appears that there is a confined unit about 12 m below the lagoon bottom. There may be a bit of leaky connectivity between the confined unit and the surface resulting in the “mixing zone” or green-colored area, but the hot colors are clearly confined from the shallower sediments and overlying surface waters. Along the west shore of the LS, there is clear evidence of either a breach or termination of the shallow freshwater zone seen down to about 6.5 m in the west. It looks as though water of higher salinity has penetrated into the lower unit (Fig. 2). Based on this evidence, it appears that groundwater flow would be more likely in the eastern ends of the lagoon (near the west side of LS).

Lagoonwide Radon Surveys

Our lagoonwide radon surveys were used to map dissolved radon distributions in the near-surface waters. All radon concentrations, based on radon-in-air measurements, were corrected for both temperature and salinity effects following the procedure of Schubert et al. (2012). There were temporal fluctuations of radon-in-water concentrations, with overall average radon amounts in LL ranging from 0.52 to 1.47 dpm l⁻¹. Salinity was inversely correlated with radon but the degree of correlation varied between sampling trips. LS provides an unquantified but small amount of low-salinity water to the lagoon, but LS waters were generally lower in radon than the eastern sections of LL.

The plots of radon concentration and salinity from each survey demonstrated substantial radon and salinity gradients across the lagoon with both ends of the lagoon having generally higher Rn and lower salinities (Fig. 3). Although the distribution patterns of radon and salinity were similar throughout the study, radon activities in general decreased throughout the investigation. Low-salinity water in the eastern part of the lagoon is derived from two freshwater inputs, SGD and LS via the canal. Radon concentrations are lower in LS and are characterized by relatively high radon in groundwater. We thus believe that there are fresh groundwater sources on the east side of the lagoon as determined by the LS resistivity and high Rn concentrations in the canals.

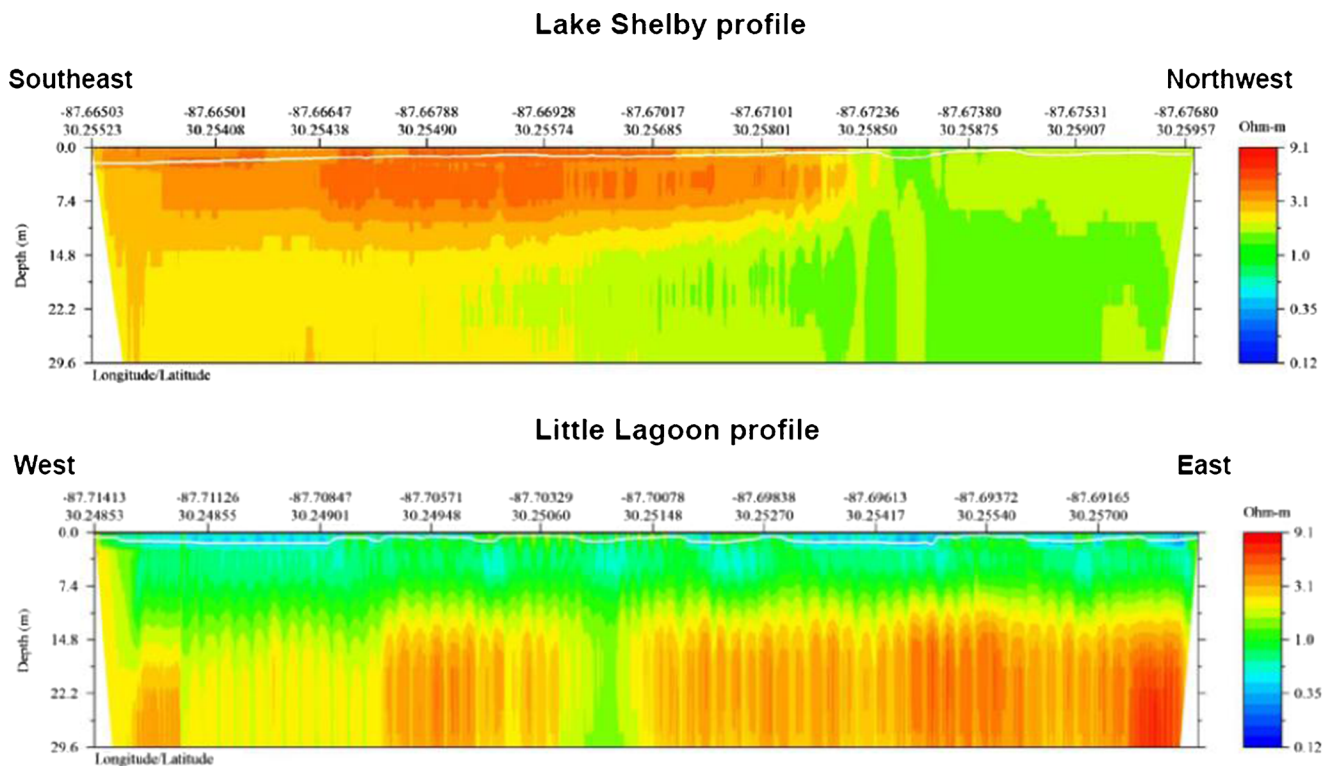
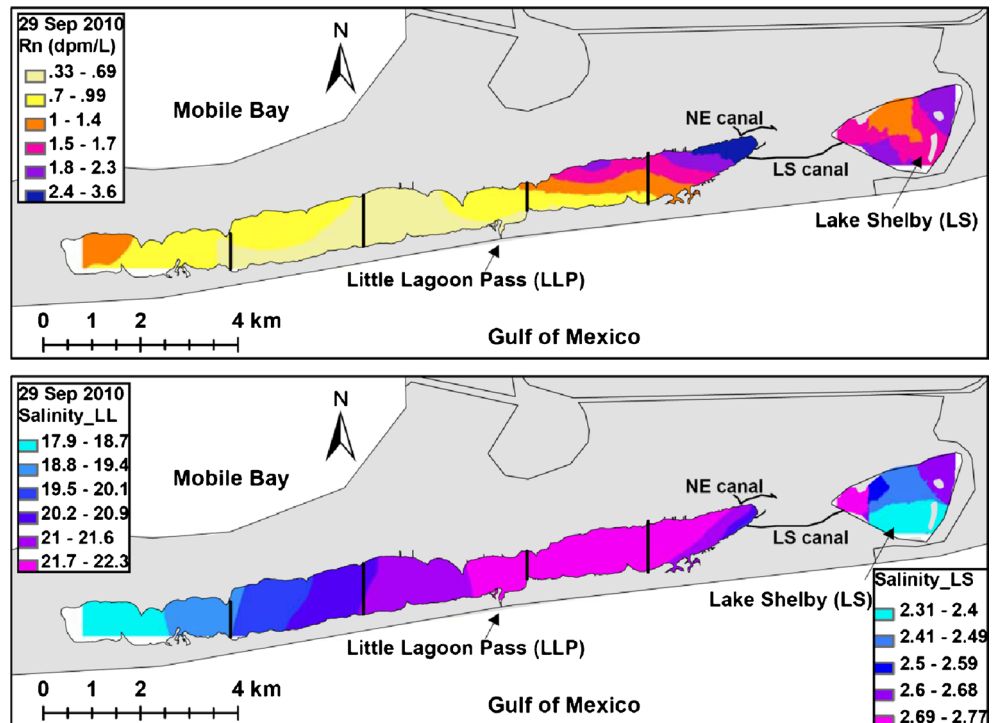


Fig. 2 Resistivity measured along the southeast shore of Little Lagoon and along the west shore of Lake Shelby on September 28–29, 2010. Note the white horizontal line is a bathymetric profile (indicates the lagoon/lake bottom)

In July 2010 and 2011, radon surveys focused on the NE and LS canals. The period in 2010 was unusual in that the LLP was closed between May 2 and July 14 to prevent oil from the

Deepwater Horizon spill entering the lagoon. There was no correlation between radon and salinity in the lagoon itself when the pass was closed, but there were strong inverse

Fig. 3 Distribution of ^{222}Rn activities (dpm l^{-1}) throughout Little Lagoon and salinity based on surveys in Little Lagoon and Lake Shelby on September 29, 2010



correlations in the canals in both 2010 and 2011 ($R > 0.8$) (Fig. 4). This suggested that freshwater entry into the NE and LS canals were important sources for radon to LL. Extrapolation of the radon-salinity trends to the y intercept (zero salinity) from these surveys produced an apparent groundwater end-member value of 29 dpm l^{-1} in July 2010, but a higher value of 56 dpm l^{-1} in July 2011. The twofold higher Rn concentrations in July 2011 relative to 2010 suggested either that there may be more than one groundwater source in the area or that the groundwater-lagoon regime may have been changed due to the closure of the pass in July 2010. After the pass was closed by backfilling with sand into LLP, the water level rose about 10–20 cm and the salinity dropped below 20 throughout the lagoon as a result of groundwater inflow and no direct communication with the GOM.

Radium Isotope Distribution in LL

As with radon concentrations, the highest radium activities were observed in the east end of the lagoon and the lowest activities were near the pass (see Supplemental Data 1 for a complete listing of all radium isotope data). Because we lack data points in the mid-salinity range, it is difficult to assess whether the distribution of Ra isotopes behaves as in a “normal” estuarine situation where radium is released by desorption from particles in the mixing zone (Fig. 5). It is evident that all of the lagoon samples are significantly enriched in ^{226}Ra over GOM waters that have an average concentration of ~ 8 dpm 100 l^{-1} (Moore & Scott 1986). Radium concentrations in the more saline canal samples were slightly higher than those in the brackish canal samples, likely due to the increase in ionic strength causing the release of Ra. The LS samples fell into a separate category with both low salinity and low radium activities.

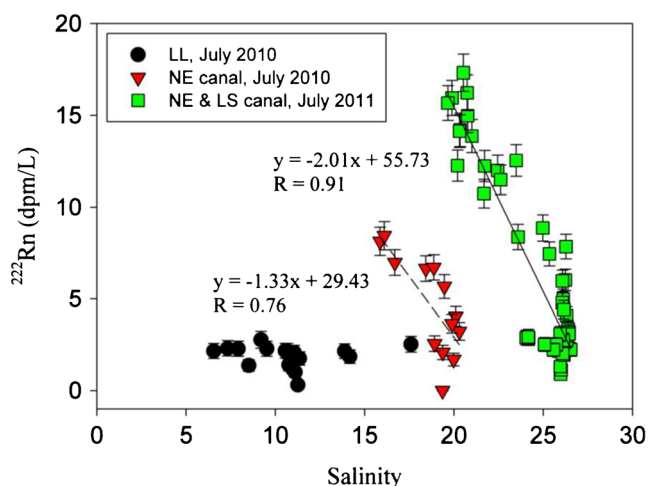


Fig. 4 ^{222}Rn vs. salinity based on survey data of the Lake Shelby and the NE canals on July 29, 2010 and July 25, 2011

We also noted that the y intercept values from the linear regression of four radium isotopes vs. salinity for the lagoon samples suggest apparent fresh groundwater end-member concentrations for ^{223}Ra , ^{224}Ra , ^{226}Ra , and ^{228}Ra of 10.8 ± 4.3 , 134 ± 5 , 56.3 ± 7.1 , and 123 ± 5 dpm 100 l^{-1} ($p < 0.01$), respectively. These values are higher than the radium activities measured in the shallow tube wells, while they are lower than the activities measured in the deeper wells. Plots of lagoon surface water and groundwater $^{223,224,228}\text{Ra}$ vs. ^{226}Ra activities showed that activity ratios (ARs) for surface lagoon waters were within the ranges found between the deep and shallow groundwaters (Fig. 6). For example, the ^{228}Ra vs. ^{226}Ra ranges of most of the samples in surface water ARs were within the range bounded by the shallow (AR = 0.5) and deep (AR = 3.3) groundwaters. Coupled with the extrapolated end-member activities from Fig. 5, this further suggests that the discharging groundwaters may represent a mixture of these two groundwater sources. The difference in groundwater Ra activities may be a difference in the mineral composition of the shallow and deeper aquifers since the mineralogy of the two aquifers is different as described earlier. The residence time of deep groundwaters is likely longer than that of the shallow groundwaters, providing more time for rock–water interactions, and chemical and physical differentiation processes. Thus, the higher radium isotope concentrations and different isotopic compositions from samples of the deep wells are not unusual.

Radon and Radium Isotopes in Groundwater

In many cases, both Rn and Ra isotopes are highly concentrated in groundwater relative to surface waters. However, the average radon concentrations in both shallow and deep groundwaters were unusually low. Radon in samples collected from the deep wells (44.0 ± 3.4 dpm l^{-1} , $n = 10$) was not significantly different ($p < 0.05$) than that measured in the shallow tube wells (52.5 ± 8.5 dpm l^{-1} , $n = 32$; Table 1 and Supplemental Data 2). While these radon activities are low compared to most groundwaters worldwide (tens to tens of thousands dpm l^{-1}), they are still 40–50 times higher than the average surface waters in LL (mean = 0.96 ± 0.71 dpm l^{-1}). In addition, the measured groundwater Rn concentrations were within the range of apparent groundwater end-member values obtained from the y intercepts in the plot of Rn vs. salinity in LS and NE canals (Fig. 4). While it is still possible that there is a mixture of shallow and deep groundwater contributing to the lagoon waters, Rn cannot differentiate the source of the groundwaters in this case.

Ra isotope activities measured in the shallow tube wells (more than half of the samples) overlapped the range of activities in the lagoon's surface waters. The groundwater radium activities in the deeper wells, however, were always much higher relative to surface waters (Supplemental Data 3).

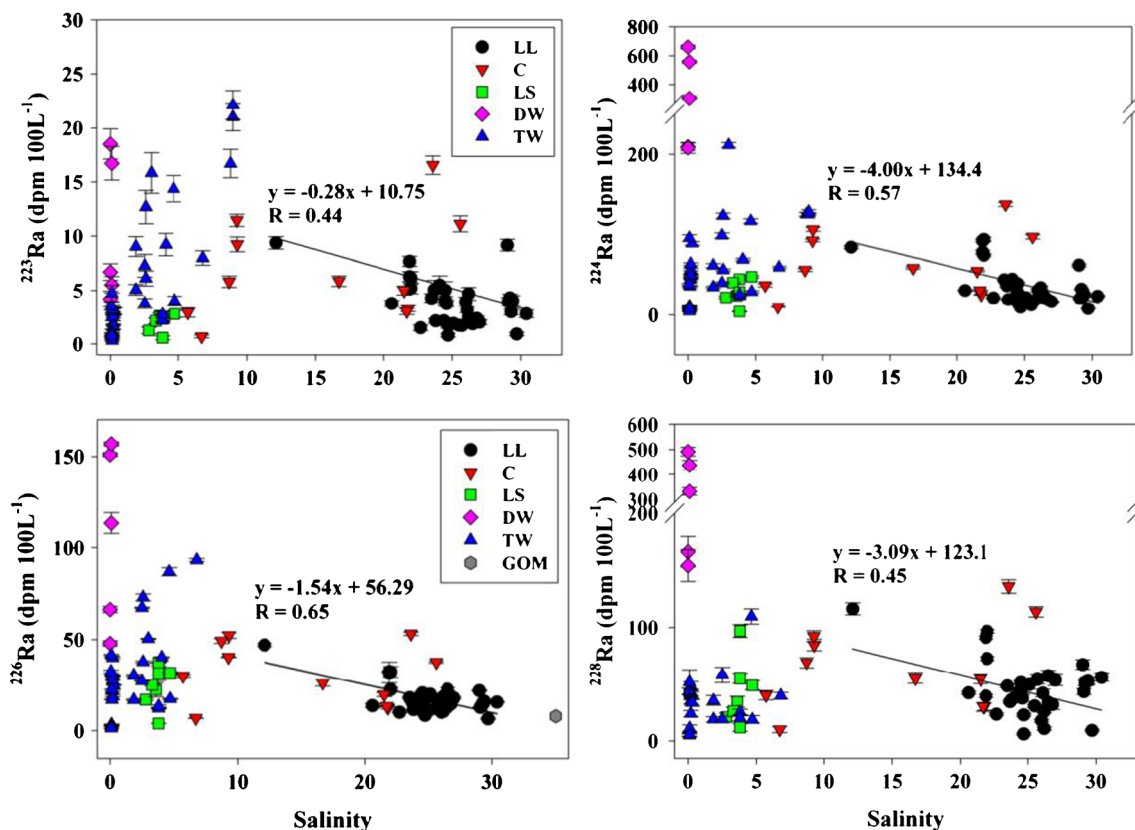


Fig. 5 Activities of ^{223,224,226,228}Ra vs. salinity from water samples in Little Lagoon (LL), canals (C), Lake Shelby (LS), deep groundwater (DW), and shallow groundwater from tube wells (TW). The solid lines

are the linear regressions for the LL samples. Note the scale breaks for the ²²⁴Ra and ²²⁸Ra plots

The average activities measured in three shallow tube wells from the eastern end of the lagoon (TW1, TW3, and TW5) were 8.63, 92.3, 49.1, and 52.4 dpm 100 l⁻¹ for ²²³Ra, ²²⁴Ra, ²²⁶Ra, and ²²⁸Ra, respectively. Deeper wells nearby contained 10.3, 388, 107, and 317 dpm 100 l⁻¹ for the same isotopes. Considering the high connectivity between the lagoon and shallow groundwaters, water in the shallow wells can more frequently undergo infiltration from the lagoon when the water table is low. Thus, it is possible that some of the shallow tube wells are occasionally recharged by low-Ra lagoon waters, especially during the drought when the water table elevation was decreasing.

Nutrients and Chlorophyll in the Lagoon and Groundwater

TN (=dissolved N + particulate N) concentrations in the lagoon's surface waters were 17.4–99.9 μM (mean 50.7±16.5 μM), TP (=dissolved P + particulate P) concentrations were 0.29–5.99 μM (mean 1.86±0.92 μM), and Si ranged from 1.6 to 130 μM (mean 43±36 μM). The TN:TP molar ratios ranged from 11.7 to 184 (mean 36.5±30.4). Concentrations of TN and silicate in groundwaters were much higher than in the surface waters of lagoon, which implies that any SGD would likely be accompanied by significant inputs

of these species. The measured groundwater TN concentrations were 359–945 μM (mean 561±271 μM), the groundwater Si ranged from 8 to 530 μM (mean 150±160 μM) and the TN:TP molar ratios were 242–853 (mean 676±371). The lagoon sediments have very high nutrient concentrations (8.8–41.2 mmol dm⁻³=mM TN; 0.7–3.8 mmol dm⁻³=mM TP) with very low N:P molar ratios (11–16).

Two of the field surveys in this study (April 2010, March 2011) were carried out during the periods when blooms of the potentially toxic diatom *Pseudo-nitzschia* spp. are most likely to occur in the GOM adjacent to LL (Liefer et al. 2009). Blooms of *Pseudo-nitzschia* spp. were observed in the lagoon itself in the years 2008–2010 (Liefer 2012). The April 2010 survey coincided with a dense, toxic bloom of *Pseudo-nitzschia* spp. (Liefer 2012; Liefer et al. 2013), while no bloom was detected during our March 2011 sampling. Microalgal abundance is estimated as chlorophyll-a (chl-a) concentration in the water column. Chl-a concentrations were two times higher in April 2010 than in March 2011, although the measured TN and TP concentrations were comparable between both sampling trips. Chl-a was highly correlated with both TN and TP in both surveys (Fig. 7).

Concentrations of TN, TP, and silicate in the lagoon's surface waters were positively correlated (0.84 < R < 0.99,

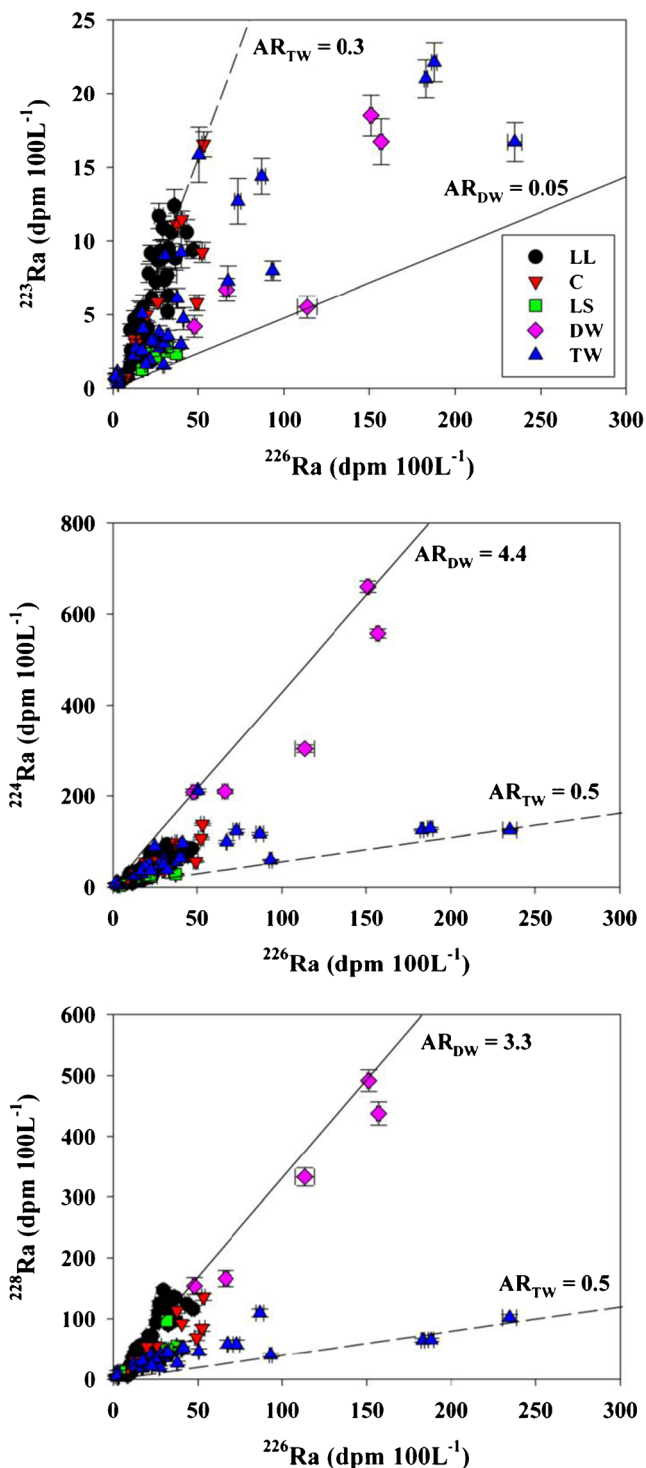


Fig. 6 Lagoon water and groundwater $^{223,224,228}\text{Ra}$ plotted against ^{226}Ra . The dashed and solid lines show the approximate ranges of activity ratios (ARs) in the shallow and deep groundwater wells, respectively

$p < 0.05$) with ex^{226}Ra in April 2010 (Fig. 8a). In contrast, none of the nutrients were significantly correlated with ex^{226}Ra in March 2011 (Fig. 8b). Silicate was negatively correlated with salinity in March 2011 ($R = -0.73$, $p < 0.05$).

Otherwise, there were no significant correlations ($p > 0.10$) between salinity and nutrient concentrations in these data sets.

Multivariate Analysis

Relationships between radioisotopes, nutrients and chl-*a*, were examined using a principal component analysis to reduce the dimensionality in these data. Data were log-transformed as needed to satisfy the requirement for normality and normalized to the mean to eliminate scale-based differences in the distributions. The distributions of data and the eigenvectors differ considerably between years (Supplemental Data 4; Fig. 9). In April 2010, there is a clear geographic separation between the east and west portions of the lagoon and the sample taken in the pass (Fig. 9a). The first principal component (PC1) explained 65 % of the variation in the data, implying that most variation is along an environmental gradient. All factors except nitrate and phosphate were significantly correlated with PC1. The second PC (PC2) explained a further 20 % of the variability for a total of 86 %. This is very high for environmental data, which is consistent with most variability being due to a common driver. Salinity and ammonium were correlated with both PC1 and PC2. Phosphate was correlated only with PC2. Nitrate was correlated only with the third PC (PC3).

The situation in March 2011 was very different. The PC1 explained only 43 % of the variability and the first two PCs combined (PC1 + PC2) explained only as much (67 %) as the PC1 did in 2010 (65 %). There was very little co-variation in the input parameters in 2011, as evidenced by the lower explanatory power of the PCs (43 vs. 65 % for PC1; 67 vs. 85 % for PC1 + PC2; Supplemental Data 4) and by the dispersion of the eigenvectors (Fig. 9b, d). The distribution of factor loadings was more diffuse in the PC biplot and the geographic clustering was less pronounced in 2011 than in 2010, indicating higher heterogeneity in the dry year (Fig. 9a, c). The majority of input parameters were correlated with two or more of the first three PCs, indicating the lack of a dominant driver of the physico-chemical variables. It is notable that the correlation between ^{224}Ra and ^{226}Ra was high in 2010 ($R = 0.79$, $p = 0.01$), while in 2011, there was no covariance between any of the isotopes ($p = 0.49$).

Discussion

Three-End-Member Mixing Model of Ra Isotopes

Theoretically, differences in the radium isotope composition can help identify different radium sources and thus we can estimate the fraction of each source using these end-member values in a mixing model. To resolve the relative end-member (A1 vs. A2 aquifers) contributions to the lagoon, we

Table 1 Summary of Ra (dpm 100 l⁻¹) and Rn (dpm l⁻¹) isotopes in the surface waters of Little Lagoon, Lake Shelby, canals and groundwater (tube and deep) wells

Site	²²³ Ra			²²⁴ Ra			²²⁶ Ra			²²⁸ Ra			²²² Rn		
	Average	S.D.	<i>n</i>	Average	S.D.	<i>n</i>	Average	S.D.	<i>n</i>	Average	S.D.	<i>n</i>	Average	S.D.	<i>n</i>
Little Lagoon	5.27	3.29	47	40.2	23.8	47	20.9	9.60	47	45.3	23.4	47	0.96	0.71	447
Lake Shelby	2.03	0.81	7	30.4	15.4	7	24.2	11.2	7	39.6	23.4	7	1.72	0.65	43
Canals	6.80	4.75	11	64.4	39.5	11	31.1	16.7	11	65.0	38.5	11	6.36	4.78	58
Tube wells	8.63	4.67	9	92.3	50.8	9	49.1	20.8	9	52.4	23.0	9	52.5	8.5	32
Deep wells	10.3	6.73	5	388	209	5	107	49.0	5	317	154	5	44.0	3.4	10

S.D. standard deviation, *n* number of samples

developed a three-end-member model similar to that used by Moore (2003) to estimate the fractions of shallow groundwater, deep groundwater and seawater using Ra isotopes as tracers. We choose ²²⁶Ra and ²²⁸Ra for the mixing model rather than ²²³Ra and ²²⁴Ra to avoid complications relating to decay. This model can help identify different radium sources and should respond well to saline flows (Moore 2003; Dulaiova & Burnett 2006). The mixing model equations used are as follows:

$$f_{SGW} + f_{DGW} + f_{SW} = 1 \tag{1}$$

$$^{226}Ra_{SGW}f_{SGW} + ^{226}Ra_{DGW}f_{DGW} + ^{226}Ra_{SW}f_{SW} = ^{226}Ra_M \tag{2}$$

$$^{228}Ra_{SGW}f_{SGW} + ^{228}Ra_{DGW}f_{DGW} + ^{228}Ra_{SW}f_{SW} = ^{228}Ra_M \tag{3}$$

where *f* is the fraction of the shallow groundwater (SGW), deep groundwater (DGW), and seawater (SW) end-members; Ra_{SGW} is ²²⁶Ra or ²²⁸Ra activity in the shallow groundwater end-member; Ra_{DGW} is ²²⁶Ra or ²²⁸Ra activity in the deep

groundwater end-member; Ra_{SW} is ²²⁶Ra or ²²⁸Ra activity in the seawater end-member; and Ra_M is measured ²²⁶Ra or ²²⁸Ra activity in the lagoon water samples. These equations can be solved for the fractions of each of the three end-members.

The concentration of Ra isotopes in discharging groundwater is an important parameter that needs to be quantitatively determined for the calculation of each fraction. The measured Ra activities in groundwater wells usually vary within a wide range due to the distribution of mineralogical and water yield properties of the aquifer as well as the groundwater salinity. In this study, the measured ²²⁸Ra/²²⁶Ra ARs had a range of 0.74–5.0 in the lagoon. This means that the ARs in different end-members (seawater, shallow, and deep groundwater) should cover such ²²⁸Ra/²²⁶Ra ARs. (i) In the three-end-member mixing model, the ARs in seawater end-member is stable at 0.7. (ii) We repeatedly sampled the shallow wells during different seasons, and we are confident that the average activities of these samples (²²⁸Ra=52.4 dpm 100 l⁻¹ and ²²⁶Ra=49.1 dpm 100 l⁻¹) can provide a reasonably good estimation of the ARs for shallow groundwater, which is 1.1. (iii) For the deep wells with a limited number of samples, the ARs must be

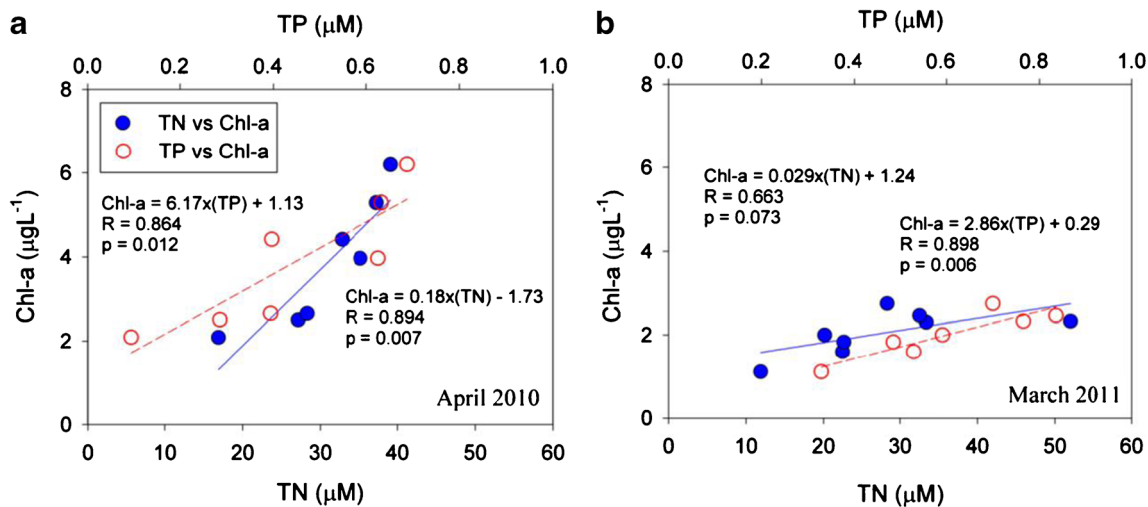


Fig. 7 Relationships between chl *a* to total nitrogen (TN) and total phosphorus (TP) in April 2010 (a) and in March 2011 (b). The solid lines are the linear regression lines for TN vs. chl *a*, and the short dashed lines are the linear regression lines for TP vs. chl *a*

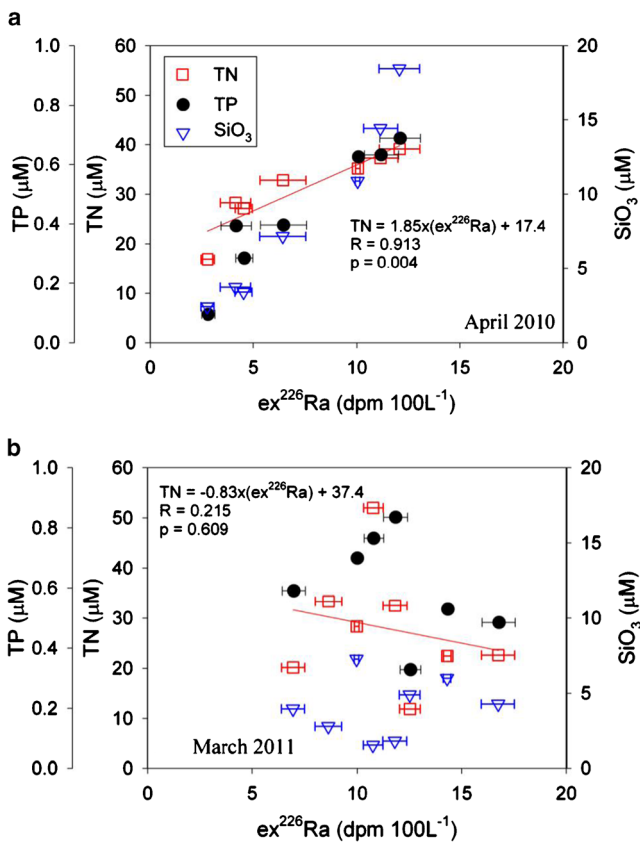


Fig. 8 Relationships between nutrient concentrations and excess radium in lagoon surface waters in April 2010 (a) and in March 2011 (b). The solid lines are the linear regression lines for TN vs. $ex^{226}\text{Ra}$

higher than 5.0 as mentioned above. The measured average ^{228}Ra activity is $317 \text{ dpm } 100 \text{ l}^{-1}$, and thus the maximum ^{226}Ra will be about $63 \text{ dpm } 100 \text{ l}^{-1}$. We found in the limited samples that ^{226}Ra varied from $47.9 \text{ dpm } 100 \text{ l}^{-1}$ (the minimum measured) to $56.0 \text{ dpm } 100 \text{ l}^{-1}$ (a little bit lower than the maximum predicted) can achieve the ARs within the range we measured in the lagoon, whereas using the higher values of ^{226}Ra generated apparent negative values for the shallow groundwater contribution for many of the lagoon samples. Extrapolation of the ^{226}Ra -salinity trend in LL waters to zero salinity also produced a value of $56 \text{ dpm } 100 \text{ l}^{-1}$ (Fig. 5), so this range seems reasonable. The error related with the selection of Ra activity in deep wells result in the uncertainty of resultant SGD of $<20\%$.

Table 2 summarizes the parameters adopted to initialize the mixing model and the corresponding results using all radium isotope data in the lagoon measured from 2010 through 2012. The average f_{SGW} , f_{DGW} , and f_{SW} were 0.10, 0.14, and 0.76, respectively. Using these fractional values, a mixture from the respective groundwater proportions gives us an average $^{228}\text{Ra}/^{226}\text{Ra}$ AR of ~ 4.1 . This value can satisfy $\sim 90\%$ ARs observed in the lagoon, indicating internal consistency with the selected groundwater end-member values.

Flushing time

Information about flushing time is essential to understand hydrodynamic processes that transport water and its constituents (Dronkers & J.T.F. Zimmerman 1982; Monsen et al. 2002). Importantly, a flushing time is necessary to convert the excess Ra into an actual SGD rate. The tidal prism method is a classical approach for estimating flushing time in tidal systems, when it can be assumed that tides dominate the flushing of the system (Dyer 1973). One may define the flushing time (T_f) for the lagoon as:

$$P = \int_H^0 A dz \quad (4)$$

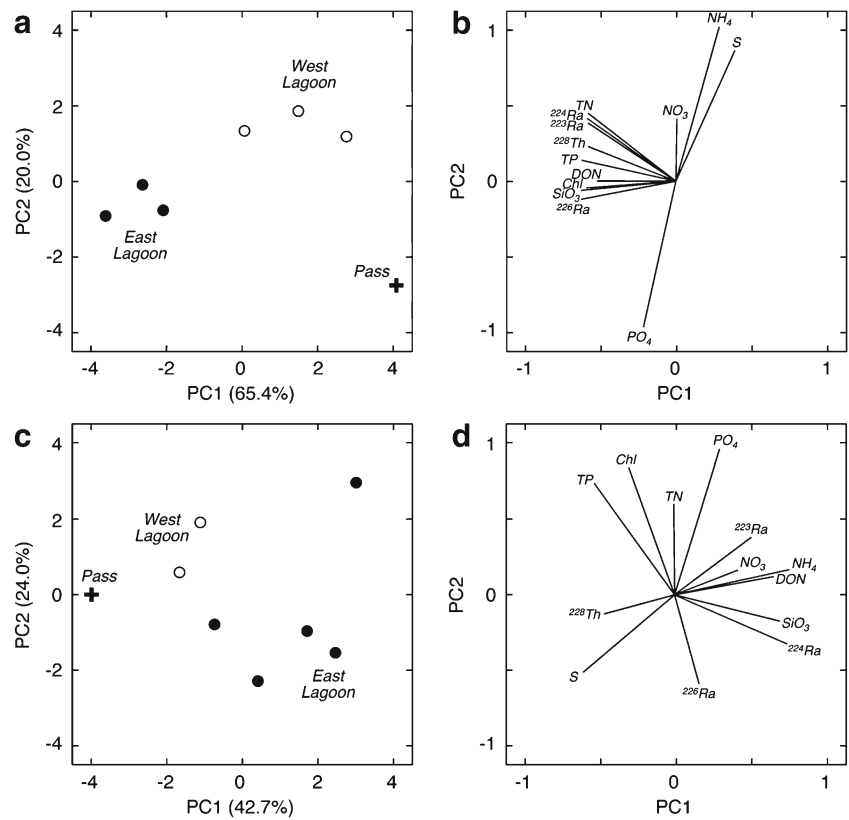
$$T_f = \frac{VT}{(1-b)P} \quad (5)$$

where P is the tidal prism, A is the water surface area of the lagoon ($10.52 \times 10^6 \text{ m}^2$), z is the average water depth over the tidal range (H), V is the volume of the lagoon (product of the surface area and average depth, $1.58 \times 10^7 \text{ m}^3$, assuming vertical walls), T is the tidal period (0.97 days), and b is the return flow factor (the fraction of effluent water that leaves the lagoon during ebb tide and returns with the next flood tide). In this model, the most difficult parameter to obtain is the return flow factor (b). Moore et al. (2006) estimated the b factor based on the difference between the outflowing ebb velocity and the incoming flood velocity as well as using a Ra isotope mixing model. In our investigation, we collected water samples during a full tidal cycle at LLP on May 21–22, 2012. We observed an inverse relationship between ^{224}Ra (and ^{223}Ra) activities and the tidal level, showing maximum Ra values at low tide and minimum values at high tide. Using ^{224}Ra (or ^{223}Ra), the b factor can be estimated as:

$$b = \frac{{}^{224}\text{Ra}_F - {}^{224}\text{Ra}_{\text{SW}}}{{}^{224}\text{Ra}_E - {}^{224}\text{Ra}_{\text{SW}}} \quad (6)$$

where $^{224}\text{Ra}_F$, $^{224}\text{Ra}_E$, and $^{224}\text{Ra}_{\text{SW}}$ are the ^{224}Ra activities measured during the flood tide, ebb tide and in seawater end-members, respectively. This approach results in a b factor that ranges from 0.02 to 0.17, lower than many other embayments in the world. This is likely due to the much slower water exchange through the shallow LLP. This b factor is similar to the range of 0.05–0.24 as determined using ^{223}Ra activities (Table 3). We also conducted radon time-series measurements at the pass. The calculated b factor based on ^{222}Rn data range from 0.02 to 0.31 without considering complications due to atmospheric evasion. The b factor can also be determined using the salinity at the pass compared to the GOM ($S_{\text{GOM}} = 35.0$), and this results in a b factor of 0.07–0.12, in the same

Fig. 9 Cross-plots of factor loadings (a, c) and Eigenvectors (b, d) for the first 2 PCs in a principal component analysis of physico-chemical parameters for April 2010 (a, b) and March 2011 (c, d). Data are identified as closed and open symbols for the eastern and western parts of the lagoon and a cross for the pass



range of Ra-derived estimates. Thus, the combined average *b* factor is 0.04–0.21.

The measured tidal amplitude for neap, mean and spring tides in the lagoon were 0.10 m, 0.15 m and 0.25 m, respectively. This allowed us to compare the flushing time for different tidal stages over an entire range of the return flow factor. The results show that the flushing time is not very sensitive to the *b* factor at these low values (Fig. 10). The T_f calculated by this approach had an error of at most 30 % when *b* increased from 0.01 to 0.3. However, small positive changes in *b* at higher values would result in much larger increases in

flushing time. Based on these calculations, the overall flushing time for LL with a *b* factor of 0.04–0.21 is estimated to be in the range of 10.1–12.3 days (mean 11.2 ± 1.1 days).

Alternatively, naturally occurring radium isotopes can be used to determine the apparent ages of coastal water masses based on an AR of a short-lived normalized to a longer-lived Ra isotope (Moore 2000). Radium that has recently entered a water body will have a higher AR that will then decrease as a function of radioactive decay and mixing. Since the mixing would be the same for both isotopes, decay time will be the dominant factor affecting the measured activities and can be

Table 2 Results of the three-end-member mixing model giving the fractions of shallow groundwater (SGW), deep groundwater (DGW) and seawater (SW) end-members in the lagoon surface waters

	²²⁶ Ra	²²⁸ Ra	Fraction SGW	Fraction DGW	Fraction SW	<i>n</i>
<i>End-members</i>						
SGW	49.1	52.4	1.00	0.00	0.00	
DGW	47.9–56.0	317	0.00	1.00	0.00	
SW	8.0	5.6	0.00	0.00	1.00	
<i>Surface water fractions</i>						
April 5, 2010	13.0	25.2	0.07	0.05	0.88	7
November 15, 2010	14.1	37.5	0.07	0.10	0.83	6
March 9, 2011	17.4	45.1	0.11	0.11	0.78	8
November 29, 2011	14.7	51.1	0.02	0.15	0.83	4
April 24, 2012	30.9	116	0.22	0.32	0.46	12
Average			0.10	0.14	0.76	37

Table 3 Estimation of return flow factor *b* based on salinity, ^{223,224}Ra and ²²²Rn differences between the outflowing ebb tide and incoming flood tide

	Flood tide	Ebb tide	Seawater Value	<i>b</i>
²²⁴ Ra (dpm 100 l ⁻¹)	10.5–14.0	33.4–43.4	9.91	0.02–0.17
²²³ Ra (dpm 100 l ⁻¹)	1.26–2.05	5.46–6.77	0.95	0.05–0.24
²²² Rn (dpm l ⁻¹)	0.1–0.3	0.8–1.1	0.08	0.02–0.31
Salinity	31.6–32.5	30.7–31.2	35.0	0.07–0.12
Average				0.04–0.21

calculated via the following expression (for the case ²²⁴Ra/²²³Ra AR):

$$\left[\frac{{}^{224}\text{Ra}}{{}^{223}\text{Ra}} \right]_{\text{obs}} = \left[\frac{{}^{224}\text{Ra}}{{}^{223}\text{Ra}} \right]_i \cdot \frac{e^{-\lambda_{224}t}}{e^{-\lambda_{223}t}} \quad (7)$$

where [²²⁴Ra/²²³Ra]_{obs} represents the measured AR of the sample, [²²⁴Ra/²²³Ra]_i is the initial AR of the radium that entered the system, λ₂₂₄ and λ₂₂₃ are the decay constants for ²²⁴Ra and ²²³Ra (λ₂₂₄=0.189 day⁻¹, λ₂₂₃=0.0606 day⁻¹), respectively, and *t* is the time since the water became enriched in Ra and was isolated from its source. Rearranging Eq. 7 allows one to solve for *t* (time):

$$\text{Ra age} = \left(\ln \left[\frac{{}^{224}\text{Ra}}{{}^{223}\text{Ra}} \right]_i - \ln \left[\frac{{}^{224}\text{Ra}}{{}^{223}\text{Ra}} \right]_{\text{obs}} \right) \times \frac{1}{\lambda_{224} - \lambda_{223}} \quad (8)$$

This approach assumes: (1) the initial ²²⁴Ra/²²³Ra (or other AR) is constant; (2) only one Ra source exists; (3) no additions or losses of Ra occur except for mixing and radioactive decay after the water leaves the source region; and (4) the open Gulf contains negligible excess ²²⁴Ra and ²²³Ra. Because the AR in the shallow and deep groundwater samples varied over a wide range, we do not have a good estimate of the initial AR.

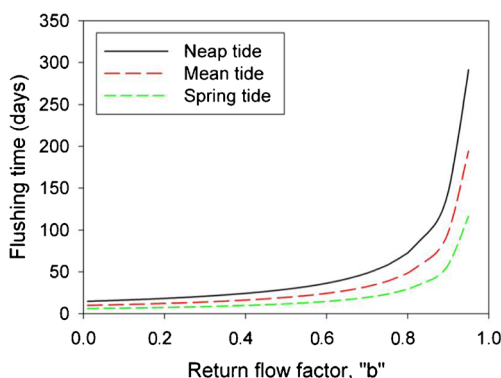


Fig. 10 Plot of estimated flushing time against the return flow factor *b* for typical neap, mean, and spring tides in Little Lagoon

Instead, we used the highest LL value measured for each suite of samples from different sampling periods to calculate relative Ra ages. Because we used the highest AR in LL rather than in the groundwater source, the calculated Ra ages are minimum estimates. However, these results will provide correct relative age differences between samples that are independent of the initial AR. Based on Eq. 8 and its assumptions, the calculated Ra ages were 2.4 days near the east end of the lagoon, and 6.2 days near the pass.

The tidal flushing model provided an overall flushing time of 11.2 days, two times higher than the maximum Ra age. To produce a radium age close to the tidal model age would require an initial ²²⁴Ra/²²³Ra AR of about 36. Our mixing model results give *f*_{SGW} and *f*_{DGW} of 0.10 and 0.14, respectively. Normalized to 100 % groundwater and ignoring the contribution through the pass, the respective groundwater fractions would be 0.42 and 0.58. Combined with the average ARs in the respective groundwaters (shallow AR = 12; deep AR = 41), we calculate a theoretical initial AR of 29 for waters that discharge into the lagoon. When we use this value in Eq. 8, we obtain an average radium age of 10 days (range = 4–14 days) for the surface waters of the lagoon, which is similar to the tidal flushing model result of 11 days.

SGD Based on ²²⁶Ra Mass Balance

Several researchers have utilized a Ra mass balance to estimate SGD rates (e.g., Moore 1996; Kim et al. 2005; Swarzenski et al. 2007). Since groundwater discharge into the lagoon is the only likely source of additional Ra, the activities of ²²⁶Ra above the baseline supported by GOM waters should represent the contribution from SGD. Assuming near-conservative behavior, the contribution of Ra which is not from the GOM waters to the lagoon can be estimated by:

$${}^{226}\text{Ra}_{\text{ex}} = {}^{226}\text{Ra}_{\text{obs}} - \left({}^{226}\text{Ra}_{\text{GOM}} \times \frac{S_{\text{obs}}}{S_{\text{GOM}}} \right) \quad (9)$$

where ²²⁶Ra_{ex} is the amount of ²²⁶Ra above that contributed by GOM waters, ²²⁶Ra_{obs} and *S*_{obs} are the measured ²²⁶Ra activity and salinity in LL samples, and ²²⁶Ra_{GOM} and *S*_{GOM} represent the known ²²⁶Ra activity and salinity in GOM waters (²²⁶Ra_{GOM} = 8.0 dpm 100 l⁻¹ and *S*_{GOM} = 35.0; Moore & Scott 1986). Because samples are not homogeneously distributed within the lagoon, an overall volume-weighted average ²²⁶Ra_{ex} is calculated based on the sampling site surface areas determined using ArcGIS maps and the average respective depth measured by our echo sounder during the surveys (Hougham et al. 2008):

$$\overline{^{226}\text{Ra}_{ex}} = \frac{\sum_{i=1}^n (^{226}\text{Ra}_{avg}^i \cdot A_i \cdot Z_i)}{A_L \cdot Z} \tag{10}$$

where *i* represents the number of each box segment (Fig. 1), *n* is the number of total boxes (5 in this case), ²²⁶Ra_{avg}^{*i*} is the average ²²⁶Ra_{ex} activity measured in each box, *A_i* is the area of each box, *A_L* is the surface area of the lagoon (10.52 × 10⁶ m²), *Z_i* is the depth of each box, and *Z* is the average depth of the entire lagoon. The calculated ²²⁶Ra_{avg}^{*i*}, areas and water depths are listed in Table 4. Using Eq. 10, the calculated ²²⁶Ra_{ex} is 9.25 dpm 100 l⁻¹ and the volume-weighted inventory of ²²⁶Ra is 131 dpm m⁻². By dividing the inventory by the derived flushing time of 11.2 ± 1.1 days, we obtained a total ²²⁶Ra flux within the system of 11.7 ± 1.15 dpm m⁻² day⁻¹. By multiplying the shallow and deep groundwater fractions (normalized to 0.42 and 0.58) by the total Ra flux, the contributions from both the A1 and A2 aquifers can be determined. The SGD flux can be calculated by:

$$\text{SGD} = \frac{\overline{^{226}\text{Ra}_{ex}} \cdot Z \cdot f_{GW}}{T_f \cdot ^{226}\text{Ra}_{GW}} \tag{11}$$

Here, ²²⁶Ra_{GW} is the ²²⁶Ra activities for either the shallow (mean 49.1 ± 20.8 dpm 100 l⁻¹) or deep (the best range consistent with the mixing model with mean of 52.0 ± 4.1 dpm 100 l⁻¹) groundwater end-members. The SGD rates calculated using this ²²⁶Ra mass balance approach were 1.0 ± 0.44 cm day⁻¹ (1.22 ± 0.53 m³ s⁻¹) for shallow groundwater and 1.3 ± 0.16 cm day⁻¹ (1.59 ± 0.20 m³ s⁻¹) for deeper groundwater (total groundwater flow of 2.81 ± 0.57 m³ s⁻¹). In this work, most of the groundwater well samples are fresh groundwater, and thus this Ra methodology gives the maximum contribution of terrestrial fresh groundwater.

SGD Based on Radon Mass Balance Model

SGD rates can also be evaluated using ²²²Rn. A one-dimensional advection–diffusion model (Cable et al. 1996)

Table 4 Summary of parameters in the overall volume-weighted average ²²⁶Ra_{ex} calculation for Little Lagoon SGD flux using a ²²⁶Ra mass balance model

Box no.	²²⁶ Ra _{avg} ^{<i>i</i>} (dpm 100 l ⁻¹)	<i>A_i</i> (10 ⁶ m ²)	<i>Z_i</i> (m)	<i>A_L</i> (10 ⁶ m ²)	<i>Z</i> (m)	$\overline{^{226}\text{Ra}_{ex}}$ (dpm 100 l ⁻¹)
1	7.78	2.13	1.53	10.52	1.42	9.25
2	6.12	2.60	1.51			
3	7.31	2.79	1.79			
4	16.5	1.69	1.06			
5	14.4	1.31	1.20			

can be set up for all inputs and outputs of ²²²Rn in the lagoon under a steady-state system to estimate groundwater discharge rate. The main principle of using natural radon to estimate SGD is based on the assumption that groundwater and diffusion from sediments are the only significant radon sources to the water column, whereas losses are via radioactive decay, atmospheric evasion and mixing of radon with low-activity seawater (Cable et al. 1996; Burnett & Dulaiova 2006; Swarzenski et al. 2007; Dimova & Burnett 2011). Radon concentrations during our lagoonwide radon surveys were all corrected for support by its parent ²²⁶Ra (mean 180 dpm m⁻³). Like ²²⁶Ra, we calculate the volume-weighted average ²²²Rn ($\overline{^{222}\text{Rn}}$) for the entire lagoon.

The relevant equations for the radon model are as follows:

$$I = \overline{^{222}\text{Rn}} \cdot Z \tag{12}$$

$$F_{adv} + F_{diff} - F_{atm} - I \cdot \lambda - I \cdot \frac{1}{T_f} = 0 \tag{13}$$

$$\text{SGD} = \frac{F_{adv} \cdot A_L}{^{222}\text{Rn}_{GW}} \tag{14}$$

where ²²²Rn_{GW} is the radon concentration in the groundwater end-member, *I* is the inventory for the volume-weighted ²²²Rn value (dpm m⁻²), *F_{adv}* is the advective flux of radon via groundwater (dpm m⁻² day⁻¹), *F_{diff}* is the diffusive flux of radon from sediments (dpm m⁻² day⁻¹), *F_{atm}* is the atmospheric evasion of radon (dpm m⁻² day⁻¹), *λ* is decay constant of ²²²Rn (0.182 day⁻¹), and 1/*T_f* is the exchange rate based on the estimated water flushing time (*T_f*). While we did not collect vertical radon profiles in the lagoon, we assumed a well-mixed water column as the water depths are mostly less than 2 m. Note that if anything, sampling radon near the surface would produce an underestimate of radon inventory and thus the calculated groundwater flow.

The total flux at the sediment–water interface should equal the Rn losses by *F_{atm}*, radioactive decay, and mixing if the system is in steady state. The loss by atmospheric evasion, *F_{atm}*, was determined using surface water temperature and salinity for the correction of the air–water partitioning of radon, and wind speed for the calculation of the gas transfer velocity (Dulaiova & Burnett 2008). The diffusion of radon from sediments, *F_{diff}*, was determined using the Rn concentration gradient between surface water and groundwater, porosity, and vertical diffusivity (Burnett et al. 2003b). We also determined the diffusive flux of radon from an experimentally defined relationship between the ²²⁶Ra content in sediments and the estimated diffusive flux of ²²²Rn. The average ²²⁶Ra activity measured from the five lagoon sediments was 0.12 ± 0.02 dpm g⁻¹. The empirical relationship between ²²²Rn flux and sediment ²²⁶Ra content (Burnett et al. 2003b) is based on

experimental data from a range of environments (both marine and fresh):

$$\text{Flux (dpm m}^{-2}\text{ day}^{-1}) = 495 \times {}^{226}\text{Ra}_{\text{sed}} + 18.2 \quad (15)$$

where ${}^{226}\text{Ra}_{\text{sed}}$ is the ${}^{226}\text{Ra}$ activity of the sediments (dpm g^{-1}). The radon diffusion calculated from Eq. 15 from surface sediments was $78 \text{ dpm m}^{-2} \text{ day}^{-1}$, which was slightly lower but comparable to the advection–diffusion model estimates of $80\text{--}98 \text{ dpm m}^{-2} \text{ day}^{-1}$. Radon fluxes in the lagoon were corrected for decay based on the Rn inventory and also corrected for mixing based on the derived average flushing time. All the input and calculated parameters for the above formulas are summarized in Table 5. It should be noted again that the Rn model does not distinguish between shallow and deep groundwaters as the concentrations were so similar. The specific lagoonwide advection rates calculated in this manner were in the range of $0.49\text{--}2.36 \text{ cm day}^{-1}$ ($0.60\text{--}2.87 \text{ m}^3 \text{ s}^{-1}$) from 2010 through 2012. These Rn-derived SGD rates from different periods overlap the average ${}^{226}\text{Ra}$ -derived SGD rates based on all our samplings (shallow + deep SGD = $2.81 \pm 0.57 \text{ m}^3 \text{ s}^{-1}$). Here, the Rn methodology is independent of salinity as radon will increase in both fresh and saline groundwaters. Together, the Rn and Ra approaches complement each other. In this area, the amount of rainfall in summer was higher than in winter from 2010 to 2012, leading to changes in the hydraulic gradient that may be reflected in groundwater seepage to the lagoon. During the majority of our study, the

southeastern USA was experiencing a severe drought, so the calculated SGD rates presented here may be lower than long-term average rates.

Temporal Variation of SGD

Based on the results from the radon surveys over the course of the study, the SGD rates decreased from May 2010 to the end of 2011, and then increased during the spring (April/June) of 2012 (Table 5; Fig. 11). The excess Rn activities in the lagoon and Rn inventories follow a trend very close to that of the calculated advection rates. The slight differences between the activity and inventory trends compared to the advection rate trend are due mainly to the corrections that are made for atmospheric evasion (dominated by temperature and wind speed variations). The decrease in SGD from May 2010 to November 2011 is likely due mainly to changes in groundwater elevation. It is clear that, except for some small variations, the overall trend of the water table was dropping from 2010 through 2011 when most of our measurements were carried out. However, the water table was clearly rising after January 2012 when the last two radon surveys were conducted. The SGD rates based on the Rn mass balance model also decreased from 2010 to 2011 and then increased during the two surveys in 2012. The higher estimated SGD rates in 2012 may be related to these two surveys being conducted shortly after unusually heavy rains in the area. We also noticed that there was relatively higher discharge from the deeper A2

Table 5 A summary of the input and calculated parameters for the entire lagoon SGD rates based on radon surveys from 2010 through 2012

	<i>Input parameters</i>					
	May 27, 2010	September 29, 2010	March 10, 2011	November 29, 2011	April 24, 2012	June 19, 2012
<i>Input parameters</i>						
Water temperature ($^{\circ}\text{C}$)	29.7	25.7	16.7	14.3	20.9	29.4
Wind speed (m s^{-1})	3.74	3.27	5.70	5.28	4.61	5.44
Water depth (m)	0.95	1.38	1.75	1.39	1.48	1.42
Rn in air conc. (dpm l^{-1})	0.07	0.07	0.07	0.07	0.07	0.07
Excess Rn in lagoon conc. (dpm l^{-1})	1.02	0.84	0.14	0.54	0.79	0.47
Rn inventory (dpm m^{-2})	969	1159	245	751	1169	667
<i>Calculated parameters</i>						
Atm. evasion ($\text{dpm m}^{-2} \text{ day}^{-1}$)	911	567	181	668	875	750
Diffusive flux ($\text{dpm m}^{-2} \text{ day}^{-1}$)	97	93	84	80	87	98
Decay ($\text{dpm m}^{-2} \text{ day}^{-1}$)	176	211	45	137	213	121
Mixing ($\text{dpm m}^{-2} \text{ day}^{-1}$)	87	103	22	67	104	60
Total flux at W.-S. int. ($\text{dpm m}^{-2} \text{ day}^{-1}$)	1,174	879	247	871	1,190	931
Specific advection (cm day^{-1})	2.3	1.7	0.49	1.7	2.4	1.9
Total discharge ($\text{m}^3 \text{ s}^{-1}$)	2.8	2.1	0.60	0.60	2.9	2.3

A steady-state advection–diffusion model (Cable et al. 1996) was used to estimate groundwater discharges. The input parameters include average measured values for temperature, wind speed, water depth, radon in air and water concentrations, and radon inventory

Estimated area of lagoon = $1.05 \times 10^7 \text{ m}^2$; measured groundwater Rn concentration = 50.4 dpm l^{-1} ; average ${}^{226}\text{Ra}$ in lagoon = 0.21 dpm l^{-1}

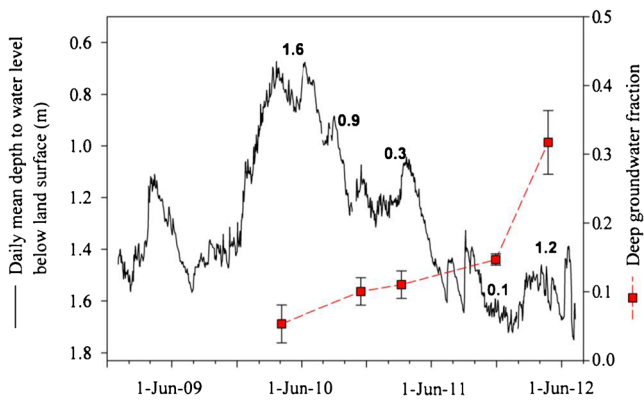


Fig. 11 The continuous line shows the shallow (A1) groundwater-level daily statistics from USGS Groundwater Monitoring Well 302416087505501 at Weeks Bay, AL (30.405°N, 87.848°W), about 18 km from Little Lagoon. Numbers next to the plot are Rn-derived SGD rates ($\text{m}^3 \text{s}^{-1}$) for the shallow aquifer. The square symbols show the fraction of deep groundwater derived from the mixing model (Table 2)

aquifer with the 2012 results having the largest deep groundwater fractions observed during the entire study (Fig. 11). If the discharge from the A2 aquifer increased during the later period of the study, perhaps due to recharge at a more distant point up-gradient from the field area, this would explain why the SGD rates in 2012 do not fit the water table trend from the A1 aquifer. Relatively higher inputs from the A2 aquifer could also have ecological consequences as the TN:TP, DON, and DIN tend to be much higher in the deeper groundwaters.

Relationship to Algal Blooms

A nutrient-limited system should show a strong correlation between chl-*a* and TN and/or TP, and we did observe this in both April 2010 and in March 2011 although the chl-*a* concentrations were lower in the later sampling (Fig. 7). In addition, a strong positive correlation was observed between nutrients and ex ^{226}Ra in April 2010 but not in March 2011, although the range in concentrations of TN and TP was similar (Fig. 8). In order to better understand what is driving these relationships, we tested for significant dependence of the PCs (Fig. 9) on the input variables using the broken-stick method (Peres-Neto et al. 2003).

In April 2010, the isotope data (^{223}Ra , ^{224}Ra , ^{226}Ra , and ^{228}Th) were all correlated exclusively with PC1, as were silicate, DON, TN, TP, and chl-*a* (Supplemental Data 4). A parsimonious explanation for this is that discharge of DON- and silicate-rich groundwater is the factor underlying PC1. TN was dominated by DON (28–66 %, mean 54 %), and TP was dominated by particulate plus dissolved organic phosphorus (71–83 %, mean 78 %). The correlation between TN and PC1 would then be because of its dominance by SGD-derived DON. The correlation between TP and PC1 might be due to discharged DOP and DIP that were rapidly assimilated into the particulate phase. Similarly, the correlation between chl-*a*

and PC1 might reflect assimilation of N and P and represent a link between SGD and phytoplankton abundance.

Although salinity was correlated with PC1, it was more highly correlated with PC2, as was ammonium, with which it was strongly and negatively correlated ($R=-0.77$, $p<0.002$). Ammonium accounted for 7–17 % (mean 11 %) of TN. It is possible that this reflects salinity-driven desorption of ammonium from DON, secondary to supply of the DON by SGD. Phosphate was correlated exclusively with PC2 and was weakly correlated with salinity ($R=0.45$, $p=0.07$). Nitrate was correlated exclusively with PC3. It accounted for only 0.4–2.1 % (mean 0.9 %) of TN.

In March 2011, the parameter grouping was much more diffuse in PC space and had a less pronounced geographic clustering. The lack of correlation between nutrient pool and the groundwater tracers indicates that multiple drivers (e.g., benthic remineralization) are responsible for the nutrients during this period and/or that there is local heterogeneity in SGD. The TN pool was even more strongly dominated by DON (59–95 %, mean 83 %) and less by ammonium (1–9 %, mean 4 %) and nitrate (0.6–1.7 %, mean 1.3 %) than in April 2010. The TP pool was comparably dominated by DOP and particulate-P (72–89 %, mean 83 %). Chl-*a* was significantly and highly correlated with TP ($R=0.90$, $p=0.006$) and weakly with TN ($R=0.66$, $p=0.07$).

The high covariance of physico-chemical parameters in 2010 suggests that their dynamics across the lagoon were responding to a common driver, namely SGD. The correlation between ^{224}Ra and ^{226}Ra , which have half-lives of 3.6 days and 1,600 years, respectively, suggests that it was relatively recent. In contrast, the low covariance of the physico-chemical parameters in 2011 and the absence of a correlation between ^{224}Ra and ^{226}Ra do not support recent discharge as a driver of systemwide structuring of the physico-chemical environment. Although the nutrient concentrations were comparable between the two years, and although chl-*a* concentrations were correlated with TN and/or TP in both years, chl-*a* concentrations were higher in 2010 than 2011. The relationship between chl-*a* and nutrient availability depends on both the rate of advection and the rate of growth vs. rates of advection and grazing (e.g., Lucas et al. 2009). The higher chl-*a* observed in 2010 might reflect taxonomic differences in pigment quotas or acclimative regulation of pigment quota to different environmental conditions (MacIntyre et al. 2002) or higher grazing pressure in 2011.

There was a bloom of the toxic diatom *Pseudo-nitzschia* spp. in the lagoon in April 2010 but not in March 2011. We have argued previously (Liefer et al. 2009; MacIntyre et al. 2011) that members of the genus that bloom in coastal waters in Alabama are opportunistic, occupying a niche characterized by recent SGD. This is consistent with the evidence for a recent flushing event in 2010 and the absence of one in 2011. There were significant differences in water temperature

between the two surveys, with a mean of 24.6 °C in 2010 vs. 16.6 °C in 2011. Dortch et al. (1997) found that the most favorable temperature for blooms of *Pseudo-nitzschia* spp. along the Louisiana/Texas shelf was 24.4±4.9 °C. Liefer et al. (2009) observed maximum densities of *Pseudo-nitzschia* spp. at 19.6±3.28 °C in Alabama waters. The temperatures observed in March 2011 were therefore well within the range in which bloom densities of *Pseudo-nitzschia* have been observed near LL (Liefer et al. 2009; MacIntyre et al. 2011), and no bloom occurred in the lagoon later in 2011 when water temperatures rose. We argue therefore that the higher groundwater discharge in April 2010 was the most likely driver of the *Pseudo-nitzschia* spp. bloom and that SGD plays a significant role in structuring the microalgal community in the lagoon.

Conclusions

This study demonstrated the utility of radon and radium isotopes in identifying areas where groundwater inputs are qualitatively important as well as quantifying SGD rates. Both resistivity and radioisotope results suggested that the strongest groundwater source was at the east end of the lagoon and associated with canals in that area. An overall water residence time (11.2±1.1 days) for the lagoon was estimated using a tidal flushing model in which the return flow factor b was calculated from $^{223,224}\text{Ra}$ data during a full tidal sampling at the LLP. The relative Ra ages based on $^{224}\text{Ra}/^{223}\text{Ra}$ ARs can also be used as a first approximation of the flushing time for the system. Since there appeared to be a mixture of shallow and deep groundwaters discharging into the lagoon, we constructed a three-end-member mixing model to calculate the fractions contributed by the two groundwater sources as well as the GOM. Combining these estimated fractions in a ^{226}Ra mass balance, this approach yielded overall average shallow and deep groundwater discharges of 1.22±0.53 and 1.59±0.20 m³ s⁻¹, respectively (total discharge = 2.81±0.57 m³ s⁻¹). SGD rates based on the Rn mass balance model ranged from 0.60 to 2.87 m³ s⁻¹ and displayed a temporal pattern in general agreement with the water table elevation in the area.

We observed well-defined relationships between nutrients and chl-*a* during both periods when there was a diatom bloom (April 2010) and when no bloom was present (March 2011). A well-defined relationship between radium (groundwater-derived) and nutrients was clear during the April 2010 sampling, while no relationship existed between the same parameters in the drier March 2011 period. A multivariate analysis was applied to examine possible relationships between SGD, nutrient concentrations, and other environmental factors. Results indicated that SGD is a likely driver of algal blooms in LL.

Acknowledgments The authors thank members of the Little Lagoon Preservation Society, especially Dennis Hatfield and George and Jean Dunn, for their continued assistance in data collection. We wish to thank C. Rocha (Trinity College, Dublin, Ireland) for his advice on the residence time calculation. This work was supported by the National Science Foundation (Grants No. OCE-0961970, 0962008, and 0961994), and the PhD Program Scholarship Fund of ECNU (2010047).

References

- Burnett, W.C., P.K. Aggarwal, A. Aureli, H. Bokuniewicz, J.E. Cable, M.A. Charette, E. Kontar, S. Krupa, K.M. Kulkarni, A. Loveless, W.S. Moore, J.A. Oberdorfer, J. Oliveira, N. Ozyurt, P. Povinec, A.M.G. Privitera, R. Rajar, R.T. Ramessur, J. Scholten, T. Stieglitz, M. Taniguchi, and J.V. Turner. 2006. Quantifying submarine groundwater discharge in the coastal zone via multiple methods. *Science of Total Environment* 367: 498–543.
- Burnett, W.C., H. Bokuniewicz, M. Huettel, W.S. Moore, and M. Taniguchi. 2003a. Groundwater and pore water inputs to the coastal zone. *Biogeochemistry* 66: 3–33.
- Burnett, W.C., J.E. Cable, and D.R. Corbett. 2003b. Radon tracing of submarine groundwater discharge in coastal environments. In M. Taniguchi, K. Wang and T. Gamo (Eds.), *Land and marine hydrogeology* (pp. 25–42). Elsevier.
- Burnett, W.C., and H. Dulaiova. 2003. Estimating the dynamics of groundwater input into the coastal zone via continuous radon-222 measurements. *Journal of Environmental Radioactivity* 69(1–2): 21–35.
- Burnett, W.C., and H. Dulaiova. 2006. Radon as a tracer of submarine groundwater discharge into a boat basin in Donnalucata, Sicily. *Continental Shelf Research* 26(7): 862–873.
- Burnett, W.C., G. Kim, and D. Lane-Smith. 2001. A continuous monitor for assessment of ^{222}Rn in the coastal ocean. *Journal of Radioanalytical and Nuclear Chemistry* 249: 167–172.
- Burnett, W.C., R. Peterson, W.S. Moore, and J. Oliveira. 2008. Radon and radium isotopes as tracers of submarine groundwater discharge—results from the Ubatuba, Brazil SGD assessment intercomparison. *Estuarine, Coastal and Shelf Science* 76: 501–511.
- Cable, J.E., W.C. Burnett, J.P. Chanton, and G.L. Weatherly. 1996. Estimating groundwater discharge into the northeastern Gulf of Mexico using radon-222. *Earth and Planetary Science Letters* 144(3–4): 591–604.
- Chandler, R.V., J.D. Moore, and B. Gillett. 1985. Ground-water chemistry and salt-water encroachment, Baldwin County. *Geological Survey of Alabama Bulletin, Alabama* 126: 16–86.
- Charette, M.A., K.O. Buesseler, and J.E. Andrews. 2001. Utility of radium isotopes for evaluating the input and transport of groundwater-derived nitrogen to a Cape Cod estuary. *Limnology and Oceanography* 46: 465–470.
- Dimova, N., and W.C. Burnett. 2011. Evaluation of groundwater discharge into small lakes based on the temporal distribution of radon-222. *Limnology and Oceanography* 56: 486–494.
- Dortch, Q., R. Robichaux, S. Pool, D. Milsted, G. Mire, N.N. Rabalais, T.M. Soniat, G.A. Fryxell, R.E. Turner, and M.L. Parsons. 1997. Abundance and vertical flux of *Pseudonitzschia* in the northern Gulf of Mexico. *Marine Ecology Progress Series* 146: 249–264.
- Dowling, D.B., R.J. Poreda, A.G. Hunt, and A.E. Carey. 2004. Ground water discharge and nitrate flux to the Gulf of Mexico. *Ground Water* 42: 401–417.
- Dronkers, J., and J.T.F. Zimmerman. (1982). Some principles of mixing in tidal lagoons. *Oceanol Acta*. Proceedings of the International Symposium on Coastal Lagoons, Bordeaux, France, 8–14 September 1981, 107–117.

- Dulaiova, H., and W.C. Burnett. 2004. An efficient method for gamma-spectrometric determination of radium-226,228 via manganese fibers. *Limnology and Oceanography: Methods* 2: 256–261.
- Dulaiova, H., and W.C. Burnett. 2006. Are groundwater inputs into river-dominated areas important? The Chao Phraya River-Gulf of Thailand. *Limnology and Oceanography* 51(5): 2232–2247.
- Dulaiova, H., and W.C. Burnett. 2008. Evaluation of the flushing rates of Apalachicola Bay, Florida via natural geochemical tracers. *Marine Chemistry* 109: 395–408.
- Dulaiova, H., R. Peterson, W.C. Burnett, and D. Lane-Smith. 2005. A multi-detector continuous monitor for assessment of ^{222}Rn in the coastal ocean. *Journal of Radioanalytical and Nuclear Chemistry* 263: 361–365.
- Dyer, K.R. (1973). *Estuaries: A physical introduction*, 2nd edn. Wiley.
- Gobler, C.J., and S.A. Sañudo-Wilhelmy. 2001. Temporal variability of groundwater seepage and brown tide blooms in a Long Island embayment. *Marine Ecology Progress Series* 217: 299–309.
- Hougham, A.L., S.B. Moran, J.P. Masterson, and R.P. Kelly. 2008. Seasonal changes in submarine groundwater discharge to coastal salt ponds estimated using ^{226}Ra and ^{228}Ra as tracers. *Marine Chemistry* 109: 268–278.
- Hu, C., F.E. Muller-Karger, and P.W. Swarzenski. 2006. Hurricanes, submarine groundwater discharge, and Florida's red tides. *Geophysical Research Letters* 33, L11601. doi:10.1029/2005GL025449.
- Kim, G., J.-W. Ryu, H.-S. Yang, and S.-T. Yun. 2005. Submarine groundwater discharge (SGD) into the Yellow Sea revealed by ^{228}Ra and ^{226}Ra isotopes: Implications for global silicate fluxes. *Earth and Planetary Science Letters* 237: 156–166.
- Laroche, J., R. Nuzzi, R. Waters, K. Wyman, P.G. Falkowski, and D.W.R. Wallace. 1997. Brown tide blooms in Long Island's coastal waters linked to interannual variability in groundwater flow. *Global Change Biology* 3: 397–410.
- Lee, Y.W., and G. Kim. 2007. Linking groundwater-borne nutrients and dinoflagellate red-tide outbreaks in the southern sea of Korea using a Ra tracer. *Estuarine, Coastal and Shelf Science* 71: 309–317.
- Lee, Y.W., G. Kim, W.A. Lim, and D.W. Hwang. 2010. A relationship between submarine groundwater-borne nutrients traced by Ra isotopes and the intensity of dinoflagellate red-tides occurring in the southern sea of Korea. *Limnology and Oceanography* 55(1): 1–10.
- Liefer, J.D. (2012). Phytoplankton Community Structure and the physiological ecology of the toxic bloom-forming diatom *Pseudo-nitzschia* spp. in coastal Alabama. Ph.D. Dissertation, University of South Alabama, Mobile, AL, May 2012.
- Liefer, J.D., H.L. MacIntyre, and W.C. Burnett. (2013). Seasonal alteration between groundwater discharge and benthic coupling as nutrient sources in a shallow coastal lagoon. *Estuaries and Coasts*, submitted for publication.
- Liefer, J.D., H.L. MacIntyre, L. Novoveská, W.L. Smith, and C.P. Dorsey. 2009. Temporal and spatial variability in *Pseudo-nitzschia* spp. in Alabama coastal waters: A "hot spot" linked to submarine groundwater discharge? *Harmful Algae* 8: 706–714.
- Lucas, L.V., J.K. Thompson, and L.R. Brown. 2009. Why are diverse relationships observed between phytoplankton biomass and transport time? *Limnology and Oceanography* 54: 381–390.
- MacIntyre, H.L., T.M. Kana, T. Anning, and R.J. Geider. 2002. Photoacclimation of photosynthesis irradiance response curves and photosynthetic pigments in microalgae and cyanobacteria. *Journal of Phycology* 38: 17–38.
- MacIntyre, H.L., A.L. Stutes, W.L. Smith, C.P. Dorsey, A. Abraham, and R.W. Dickey. 2011. Environmental correlates of community composition and toxicity during a bloom of *Pseudo-nitzschia* spp. in the northern Gulf of Mexico. *Journal of Plankton Research* 33: 273–295.
- Monsen, N.E., J.E. Cloern, L.V. Lucas, and S.G. Monismith. 2002. A comment on the use of flushing time, residence time, and age as transport time scales. *Limnology and Oceanography* 47: 1545–1553.
- Moore, D.G., and M.R. Scott. 1986. Behavior of Ra-226 in the Mississippi River mixing zone. *Journal of Geophysical Research: Oceans* 91(12): 14317–14329.
- Moore, W.S. 1976. Sampling ^{228}Ra in the deep ocean. *Deep Sea Research-Oceanography Abstract* 23: 647–651.
- Moore, W.S. 1996. Large groundwater inputs to coastal waters revealed by ^{226}Ra enrichments. *Nature* 380: 612–614.
- Moore, W.S. 2000. Determining coastal mixing rates using radium isotopes. *Continental Shelf Research* 20: 1993–2007.
- Moore, W.S. 2003. Sources and fluxes of submarine groundwater discharge delineated by radium isotopes. *Biogeochemistry* 66: 75–93.
- Moore, W.S. 2010. The effect of submarine groundwater discharge on the ocean. *Annual Review of Marine Science* 2: 59–88. doi:10.1146/annurev-marine-120308-081019.
- Moore, W.S., and R. Arnold. 1996. Measurement of ^{223}Ra and ^{224}Ra in coastal waters using a delayed coincidence counter. *Journal of Geophysical Research* 101(C1): 1321–1329.
- Moore, W.S., J.O. Blanton, and S.B. Joye. 2006. Estimates of flushing times, submarine groundwater discharge, and nutrient fluxes to Okatee Estuary, South Carolina. *Journal of Geophysical Research* 111, C09006. doi:10.1029/2005JC003041.
- Murgulet, D., and G.R. Tick. 2008. The extent of saltwater intrusion in southern Baldwin County, Alabama. *Environmental Geology* 55: 1235–1245.
- Murgulet, D., and G.R. Tick. 2009. Assessing the extent and sources of nitrate contamination in the aquifer system of southern Baldwin County, Alabama. *Environmental Geology* 58: 1051–1065.
- Peres-Neto, P.R., D.A. Jackson, and K.M. Somer. 2003. Giving meaningful interpretation to ordination axes: Assessing loading significance in principal component analysis. *Ecology* 84: 2347–2363.
- Peterson, R.N., W.C. Burnett, N. Dimova, and I.R. Santos. 2009. Comparison of measurement methods for radium-226 on manganese-fiber. *Limnology and Oceanography-Methods* 7: 196–205.
- Santos, I.R., W.C. Burnett, J.P. Chanton, B. Mwashote, I.G.N.A. Suryaputra, and T. Dittmar. 2008a. Nutrient biogeochemistry in a Gulf of Mexico subterranean estuary and groundwater-derived fluxes to the coastal ocean. *Limnology and Oceanography* 53(2): 705–718.
- Santos, I.R., F. Niencheski, W.C. Burnett, R. Peterson, J. Chanton, C.F.F. Andrade, I.B. Milani, A. Schmidt, and K. Knoeller. 2008b. Tracing anthropogenically driven groundwater discharge into a coastal lagoon from southern Brazil. *Journal of Hydrology* 353: 275–293.
- Schubert, M., A. Paschke, E. Lieberman, and W.C. Burnett. 2012. Air–water partitioning of ^{222}Rn and its dependence on water temperature and salinity. *Environmental Science and Technology* 46(7): 3905–3911.
- Slopp, C.P., and P. Van Cappellen. 2004. Nutrient inputs to the coastal ocean through submarine groundwater discharge: Controls and potential impact. *Journal of Hydrology* 295: 64–86.
- Solórzano, L., and J.H. Sharp. 1980. Determination of total dissolved phosphorus and particulate phosphorus in natural waters. *Limnology and Oceanography* 25: 754–758.
- Swarzenski, P.W., W.C. Burnett, W.J. Greenwood, B. Herut, R. Peterson, N. Dimova, Y. Shalem, Y. Yechieli, and Y. Weinstein. 2006a. Combined time-series resistivity and geochemical tracer techniques to examine submarine groundwater discharge at Dor Beach, Israel. *Geophysical Research Letters* 33, L24405. doi:10.1029/2006GL028282.
- Swarzenski, P.W., W.H. Orem, B.F. McPherson, M. Baskaran, and Y.S. Wan. 2006b. Biogeochemical transport in the Loxahatchee River estuary, Florida: the role of submarine groundwater discharge. *Marine Chemistry* 101(3–4): 248–265.
- Swarzenski, P.W., C. Reich, K.D. Kroeger, and M. Baskaran. 2007. Ra and Rn isotopes as natural tracers of submarine groundwater discharge in Tampa Bay, Florida. *Marine Chemistry* 104: 69–84.
- Taniguchi, M., T. Ishitobi, W.C. Burnett, and G. Wattayakorn. 2007. Evaluating ground water–sea water interactions via resistivity and seepage meters. *Ground Water* 45(6): 729–735.

- Valderrama, G.C. 1981. The simultaneous analysis of total nitrogen and total phosphorus in natural waters. *Marine Chemistry* 10: 109–122.
- Valiela, I., J. Costa, K. Foreman, J.M. Teal, B. Howes, and D. Aubrey. 1990. Transport of groundwater-borne nutrients from watersheds and their effects on coastal waters. *Biodegradation* 10: 177–197.